

BP-Net: Cuff-less, Calibration-free, and Non-invasive Blood Pressure Estimation via a Generic Deep Convolutional Architecture

Soheil Zabihi[‡], Elahe Rahimian[†], Fatemeh Marefat[†], Amir Asif[‡], Pedram Mohseni[†], and Arash Mohammadi[†]

[‡] *Electrical and Computer Engineering, Concordia University,
1455 De Maisonneuve Blv. W., EV-009.187, Montreal, QC, Canada, H3G-1M8*

[†] *Concordia Institute for Information Systems Engineering, Concordia University*

[†] *Electrical, Computer, and Systems Engineering, Case Western Reserve University, Cleveland, OH, USA
Emails: {s_zab, arashmoh, e_ahimia}@encs.concordia.ca*

Abstract

Objective: The paper focuses on development of robust and accurate processing solutions for continuous and cuff-less blood pressure (BP) monitoring. In this regard, a robust deep learning-based framework is proposed for computation of low latency, continuous, and calibration-free upper and lower bounds on the systolic and diastolic BP. *Method:* Referred to as the BP-Net, the proposed framework is a novel convolutional architecture that provides longer effective memory while achieving superior performance due to incorporation of casual dilated convolutions and residual connections. To utilize the real potential of deep learning in extraction of intrinsic features (deep features) and enhance the long-term robustness, the BP-Net uses raw Electrocardiograph (ECG) and Photoplethysmograph (PPG) signals without extraction of any form of hand-crafted features as it is common in existing solutions. *Results:* By capitalizing on the fact that datasets used in recent literature are not unified and properly defined, a benchmark dataset is constructed from the MIMIC-I and MIMIC-III databases obtained from PhysioNet. The proposed BP-Net is evaluated based on this benchmark dataset demonstrating promising performance and shows superior generalizable capacity. *Conclusion:* The proposed BP-Net architecture is more accurate than canonical recurrent networks and enhances the long-term robustness of the BP estimation task. *Significance:* The proposed BP-Net architecture addresses key drawbacks of existing BP estimation solutions, i.e., relying heavily on extraction of hand-crafted features, such as pulse arrival time (PAT), and; Lack of robustness. Finally, the constructed BP-Net dataset provides a unified base for evaluation and comparison of deep learning-based BP estimation algorithms.

Keywords: Continuous Blood Pressure (BP) Estimation, Deep Learning, Electrocardiograph

(ECG), Photoplethysmograph (PPG).

1. Introduction

An alarming population ageing is widely expected in near future partially due to recent advancements of biomedical health technologies. According to a recent publication by the United Nation [1], the number of seniors over the age of 60 is expected to double by 2050, even it is projected that population of seniors will be more than population of minors/youth at ages 10-24 by 2050. Consequent of this inevitable worldwide population aging trend is significant increase in age-related health issues, in particular cardiovascular conditions. According to World Health Organization report and in a global scale, cardiovascular diseases account for approximately 17 million loss of lives annually, which accounts for one third of the total deaths around the world. Of these, complications of hypertension account for 9.4 million loss of lives annually. These facts call for an urgent quest to develop advanced continuous monitoring, efficient diagnosis, and timely treatment of cardiovascular conditions. The paper focuses on the former category, i.e., continuous monitoring of Blood Pressure (BP), which is a widely measured physiological characteristic used to indicate cardiovascular health status of an individual.

Generally speaking, BP can be described as the pressure applied by blood to the arteries (wall of the blood vessels) ranging between two limits, i.e., a maximum value named Systolic Blood Pressure (SBP) to a minimum value referred to as the Diastolic Blood Pressure (DBP). A person is diagnosed by hypertension when her/his SBP goes above 140mmHg and the DBP reaches above 90 mmHg. The BP, however, varies significantly over time [2] as the result of different environmental factors such as stress, mental situations, and food consumption to name but a few. This necessitates continuous monitoring of BP to assist in early detection and diagnosis of hypertension conditions together with devising accurate treatments to reduce overall mortality rate of patients suffering from hypertension. While regular BP checkups are recommended by physicians for seniors, this typically can not be achieved due to complications of human activities and fast pace of modern life style, furthermore, historical data shows that on average 20% of seniors have higher measured BP at clinics in comparison to relaxed home environment. Consequently, continuous and in-home monitoring of BP [3]-[6] via utilization of advanced Biological Signal Processing (BSP), Artificial Intelligence (AI) and Machine Learning (ML) techniques [7]-[12] becomes of paramount importance

and is the focus of the paper. In Section 2, we provide an overview of recent literature in this domain to better position the contributions of the paper (outlined below), and motivate the need for development of the proposed BP-Net architecture.

Contributions: The paper proposes a novel deep learning framework, referred to as the BP-Net, that addresses the identified drawbacks of existing solutions. More specifically, we propose a novel convolutional architecture for estimating BP. After denoising the photo-plethysmograph (PPG) and electrocardiogram (ECG) signals [13], the pre-processed signals are provided as inputs to the designed convolutional architecture, i.e., excluding the need for feeding the models with hand-crafted features, therefore, utilizing the intrinsic deep features of the PPG and ECG signals. In brief, the main contributions of the paper can be summarized as follows:

- Most of the existing data-driven methodologies proposed for cuff-less BP estimation depend on extraction of specific hand-crafted features such as pulse arrival time (PAT) [15]-[23]. Capitalizing on recent evidence that neural networks can extract the necessary features automatically without the need for complex feature engineering, we propose a convolutional architecture model that extracts necessary features automatically using raw ECG and PPG waveforms. The proposed model is able to estimate BP with high accuracy in an end-to-end manner.
- The proposed BP-Net provides longer effective memory while achieving superior performance in comparison to recurrent neural networks due to incorporation of casual dilated convolutions and residual connections.
- In the studies presented so far, the type of ECG signal is not considered (i.e., the BP is estimated based on one type of ECG). Availability of different types of ECG signals (which is not the same for every subject) makes it difficult to evaluate the generality of the obtained results. To address this problem, and also to show the generality of the proposed model, we use different types of ECG signals such as I, II, III, and IV.
- By capitalizing on the significant importance of continuous BP monitoring and the fact that datasets used in recent literature are not unified and properly defined, a benchmark data set is constructed from the MIMIC-I and MIMIC-III databases from PhysioNet to provide a unified base for evaluation and comparison of deep learning-based BP estimation algorithms.

The rest of the paper is organized as follows: Section 2 outlines recent continuous BP estimation solutions and motivates the need for development of the proposed BP-Net architecture. The proposed BP-Net architecture is then presented in Section 3. Section 4 presents the experimental results for the evaluation of the proposed framework based on real constructed datasets. Finally, Section 5 concludes the paper.

2. Related Works

Generally speaking, when it comes to measuring BP, commonly, either a cuff-based approach is utilized, which provides upper arm BP measurements, or one resorts to cuff-less (possibly invasive) solutions. Upper arm BP monitoring can provide users with an indirect and non-continuous BP measurement technique by using an inflatable cuff and stethoscope. Such cuff-based methods suffer from several drawbacks including: (i) Being inconvenient and unhealthy especially in public places; (ii) Require proper training prior to utilization; (iii) Not being ideal for self-use and long-term monitoring of BP, and; (iv) Being incapable of providing continuous BP measurements [2]. Cuff-less BP monitoring [14], on the other hand, eliminates the common uncomfortable factors associated with the former category and has the potential to continuously provide BP estimates without using any inflatable cuff.

Recently, there has been a great surge of interest towards the goal of performing continuous BP monitoring via *Physiologically Inspired Models* [15]-[18] in particular pulse transit time (PTT) and pulse arrival time (PAT). The PAT, sum of PTT and pre-ejection period, is considered as the main marker of BP for development of cuff-less BP estimation algorithms due to its simple measurement procedure. The PAT [19, 20] is defined as the time required for a heart beat to transfer to a body peripheral and has a tight relationship (correlation) to the BP. The existing correlation between PAT and BP, although well established, is highly non-linear depending on several uncertain factors varying across different individuals and over time [21, 22]. Therefore, there has been different attempts [17]-[23] to construct calibration models to account for such variations. In calibration-based models, the focus is on extracting meaningful features to be fed to processing and learning models. Such models, however, are applicable only for use in short intervals such as exercise tests. Existing methods for cuff-less and continuous BP estimation can be classified into the following two main categories:

(i) Hand-crafted Regression-based Models: Models belonging to this category are developed by extracting hand-crafted features and exploiting various conventional BSP and ML algorithms such as decision trees (DT), support vector regression (SVR), shallow neural networks, and Bayesian linear regression (BLR) to name but a few. Typically, PPG and ECG signals are used jointly [2, 24] to extract PAT features to construct a regression model for estimating the BP. In Reference [25], for instance, a linear regression model (i.e., the SVR) is coupled with a radial basis function (RBF) kernel, and a single hidden layer neural network with a linear output to estimate the BP.

The key drawback of the aforementioned conventional methods is that such models rely heavily on extraction of hand-crafted features, such as PAT, and directly map the given input into the target value while ignoring the critical temporal dependencies in the BP dynamics. This could be considered as the root of long-term inaccuracy of such models, and results in lack of robustness due to strong dependencies on the calibration parameters and the choice of hand-crafted features to describe the signal for subsequent regression [26]. Lack of robustness translates into accuracy decay over time requiring frequent calibrations, especially for multi-day continuous BP prediction tasks. Robustness is essential for use of developed models in clinical settings, therefore, lack of robustness of existing solutions has limited their practical utilization.

(ii) Deep Learning-based Models: While research works on hand-crafted and regression-based models are extensive, deep-learning based BP estimation [27, 28] is still in its infancy. In deep-learning models, commonly, hand-crafted features (e.g., extracted PAT features) are fed to neural network models such as long short term memory (LSTM) models, recurrent neural networks (RNN), convolutional neural networks (CNN), or bidirectional RNN (BRNN). For instance, Reference [27] proposed to formulate BP prediction as a sequence learning problem, and proposed a deep RNN model, which is targeted for multi-day continuous BP prediction. The RNN model works with a set of seven representative hand-crafted features extracted from ECG and PPG signals. Another recent example is Reference [29], where the authors proposed a waveform-based Artificial neural network (ANN)-LSTM model. The model consists of a hierarchical structure where the lower hierarchy level uses ANNs to extract the required features from the ECG/PPG waveforms, while the upper hierarchy level uses stacked LSTM layers to learn the time domain variations of the features extracted in the lower hierarchy level.

One can identify two key drawbacks associated with the limited deep learning-based models

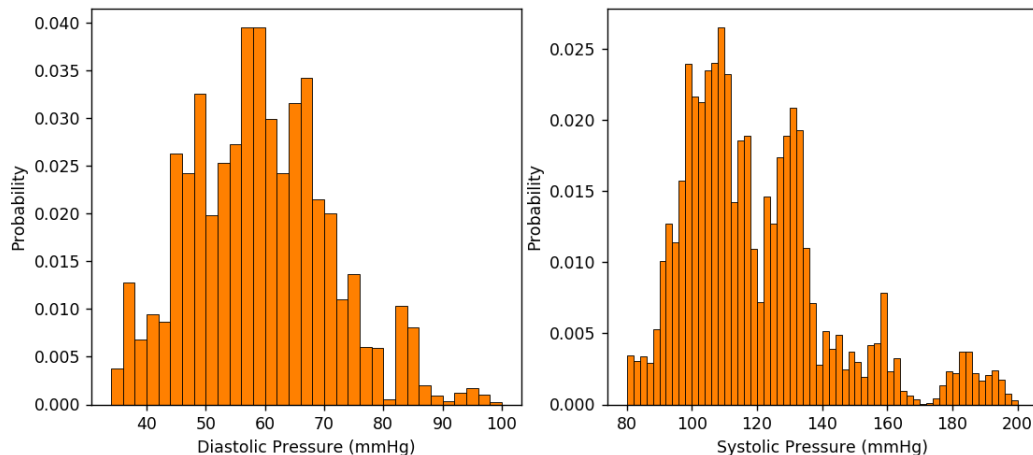


Figure 1: Histogram of the preprocessed database. (a) Diastolic blood pressure. (b) Systolic blood pressure.

developed recently for BP estimation: (a) In most of the studies presented so far, before extracting the deep features, representative hand-crafted features of input signals are first selected/extracted, which are then used to train a deep neural network. In other words, such methods ignore the real potential of deep learning in utilizing the intrinsic features (deep features) of the input signals, and; (b) Lack of a benchmark dataset for evaluation and comparison of developed deep learning-based BP estimation algorithms. In other words, datasets used in recent literature are not unified and properly defined, which makes evaluations and comparison difficult. Commonly a subset of MIMIC-I or MIMIC-III databases from PhysioNet is used without providing details on the training, validation, and test sets rendering reproducibility and fair comparisons impossible. In some cases, results evaluated based on two different datasets are compared, which can not be considered as a fair base for evaluation purposes. Furthermore, commonly a limited number of subjects within specific age/gender group is used making it difficult to evaluate the generality of the obtained results across different characteristics.

To alleviate the aforementioned identified shortcomings of existing continuous BP estimation solutions, next we present the proposed BP-Net architecture.

3. The BP-Net Framework

In this paper, estimation of the SBP and the DBP is performed automatically via extraction of deep-features from ECG and PPG signals without incorporation of any form of hand-crafted PAT

features. To achieve this goal, we approach the BP estimation problem as a sequence modelling task. Before describing the architecture of the proposed BP-Net, in what follows, first we provide a brief overview of the constructed dataset and pre-processing pipelines utilized to develop the proposed BP-Net.

3.1. BP-Net Dataset

As stated previously, the paper introduces a unified and properly defined benchmark dataset given the significant importance of continuous BP monitoring and the fact that recent research works train and test their algorithms on datasets of their choice, impeding a fair judgment between their solutions. Capitalizing on this issue, we aim to provide a platform with reference dataset, where different algorithms can be evaluated and compared by utilizing the same training set to optimize new processing algorithms, and the same test dataset to be used to measure the associated performance. Despite the differences, all existing studies share a common validation procedure in which experiments are conducted on a proprietary database containing fewer number of subjects with reference to our work, therefore, it is difficult to evaluate the generality of the obtained results across gender and age. For this purpose, we increased the number of subject (104 individuals), and show that this increase in the number of subjects with respect to prior works can lead to challenging issues in terms of classification accuracy and generality across subjects.

The BP-Net dataset is collected from the Multi-parameter Intelligent Monitoring for Intensive Care (MIMIC) [30] provided by PhysioNet server. MIMIC-I database contains PPG, multi-lead ECGs, and arterial blood pressure (ABP) signals at 125 samples per second with 8 bit precision. Data is derived from 90 patients monitors in the medical, surgical, and cardiac intensive car units (ICU) of different hospitals [30]. The requirement set froward to construct the BP-Net dataset is to have concurrent PPG, ECG, and ABP signals, therefore, out of the 90 available subjects, we were able to collect data from 56 patients. To further increase the number of subjects, MIMIC-III [30] database, which is an update to the common MIMIC-II, is also used as the second source for data preparation. The MIMIC-III contains data associated with a large number of different hospitals for distinct patients in ICU between 2001 and 2012. Similar to MIMIC-I, signals were sampled at the frequency rate of 125 Hz with 8 bit accuracy [30]. We have collected data from 48 patients who had simultaneous PPG, ECG, and ABP from this dataset resulting in total of 104 subjects in the BP-Net dataset. The BP distribution histograms are shown in Fig. 1. After preparing the

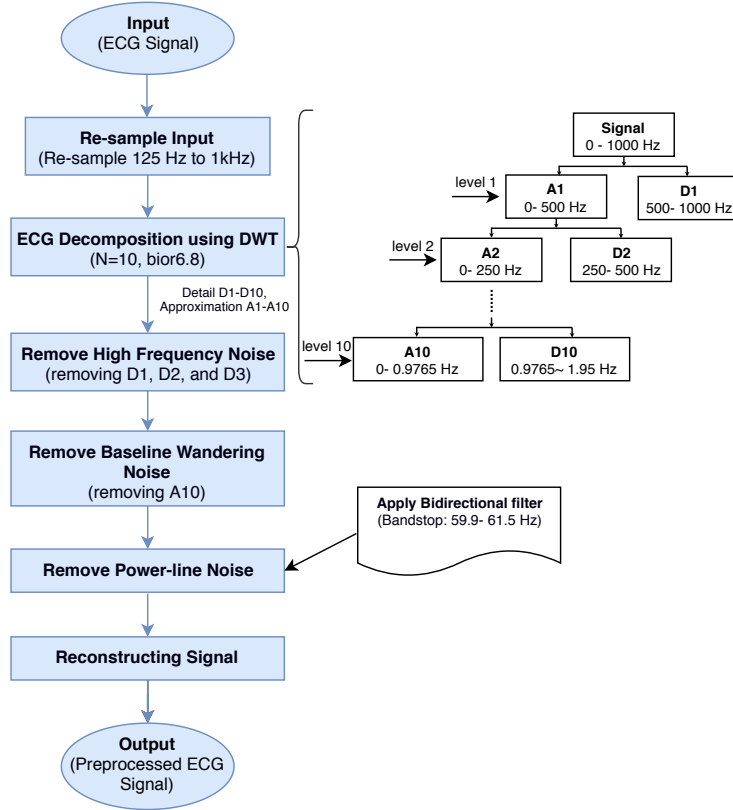


Figure 2: Raw signal pre-processing pipeline.

input and output for the model, the data for each patient is divided into 70% for training, 10% for validation and 20% for test. The constructed BP-Net dataset including train, validation and test subsets are available through its web-page: <http://i-sip.encs.concordia.ca/datasets.html>.

3.2. Preprocessing

Before describing details of the proposed BP-Net for BP estimation, in this sub-section we present the essential pre-processing steps performed on ECG and PPG signals. Generally speaking, the ECG signals are contaminated by different noise and artifact sources [2]-[32] such as high frequency noise (e.g., electrosurgical noise, muscle contraction noise), power line interference noise (50 Hz or 60 Hz), and low frequency noises (e.g., baseline wandering noise, motion artifacts affected by skin-electrodes). A great number of methods are introduced in the literature to remove noise/artifacts from ECG signals including Kalman filter-based methodologies [33, 34], filtering techniques (IIR or FIR filters), adaptive noise cancellation, empirical mode decomposition techniques, variational mode decomposition, and discrete wavelet decomposition (DWT) [35]. Although each of the such techniques has its pros and cons, in this work, the DWT technique [36] is applied

to remove noise from signals since in contrary to other methods, it can be applied to non-stationary signals without introducing any artificial information to the original signal.

By implementing the pre-processing block shown in Fig. 2, each ECG signal is denoised and prepared as an input for the proposed BP-Net architecture. The first step for filtering ECG signals is up-sampling the frequency from 125 Hz to 1,000 Hz, which makes it stable to possible changes of the sampling frequency. Then, by applying *Biorthogonal 6.8 (bior6.8)* mother wavelet with 10 decomposition levels, the signal is decomposed into approximation and detail components denoted by $D1$ - $D10$ and $A1$ - $A10$ to refer to the detailed, and approximation components, respectively. The detailed coefficients $D1$, $D2$, and $D3$, contain high frequency noises such as muscle contraction [31], which are discarded as the next step. Then Approximation coefficient $A10$ is eliminated because it contains low frequency noises, which are caused by respiration, and body movements (this noise can be seen as a sinusoidal component). After that, a *bidirectional* filter is used to suppress the 60Hz power-line interference noise using a bandstop filter (59.5 - 61.5 Hz). Finally, the signal is reconstructed by Inverse DWT (IDWT). We applied an approach of similar nature to the above discussion to pre-process PPG signals and remove potential noisy contaminations.

3.3. The BP-Net Architecture

We consider the problem of BP estimation from ECG and PPG signals collected from $N_s = 104$ number of subjects, where ECG, PPG, and ABP data associated with subject l , for $(1 \leq l \leq N_s)$, each has total of $T^{(l)}$ number of samples. We define an ECG vector $\mathbf{x}^{(l)}(t) = [X_1^{(l)}, \dots, X_t^{(l)}]^T$ consisting of samples from ECG time-series collected from the l^{th} subject from the starting time ($t = 1$) to time ($t \leq T^{(l)}$). Note that $\mathbf{x}^{(l)}(T^{(l)})$ is a vector representing all ECG samples available for the l^{th} subject. Similarly, we define a PPG vector $\mathbf{p}^{(l)}(t) = [P_1^{(l)}, \dots, P_t^{(l)}]^T$ representing PPG measurements collected from the l^{th} individual upto and including time ($t \leq T^{(l)}$). Finally, vector $\mathbf{b}^{(l)}(t) = [B_1^{(l)}, \dots, B_t^{(l)}]^T$ represents the BP values from time instant 1 to t .

The goal of the BP-Net architecture is to learn a nonlinear function $\mathbf{h}(\mathbf{x}^{(l)}(t), \mathbf{p}^{(l)}(t))$ that takes as input ECG $\mathbf{x}^{(l)}(t)$ and PPG $\mathbf{p}^{(l)}(t)$ sequences and provides a predicted value $\hat{B}(t)$ for the BP at time t . One limitation is that the predicted BP output, $\hat{B}(t)$, at time step t only depends on the input data obtained prior to time t , i.e., there is no leakage of information from future into the past. The target of network is to minimize the cost function $\mathcal{L}(B(t), \mathbf{h}(\mathbf{x}^{(l)}(t), \mathbf{p}^{(l)}(t)))$ between all the results of the hypothesized functions $\mathbf{h}(\cdot)$ with ECG and PPG input sequences, and the actual

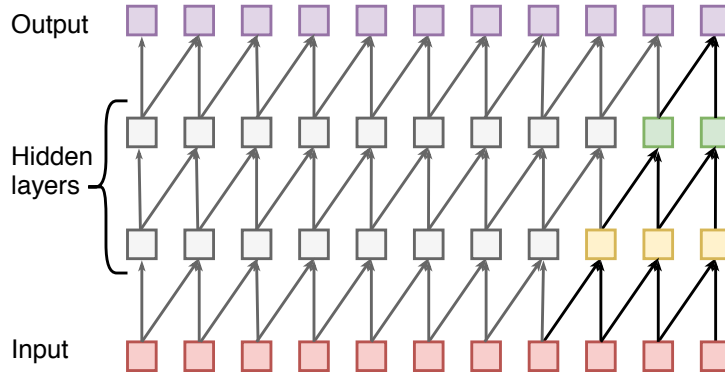


Figure 3: An example of a Causal Convolution.

output $B(t)$. In what follows, we describe different aspects of the proposed BP-Net architecture.

Casual Convolutions: As stated above, a basic aspect of the proposed BP-Net architecture is that we want to make sure that the output $\hat{B}(t)$ estimated at time step t depends only on previous input samples (i.e., ECG $\mathbf{x}^{(l)}(t)$ and PPG $\mathbf{p}^{(l)}(t)$ sequences) and not on any “future” values. In other words, while during the training phase, we have access to future values of the input signals (ECG and PPG sequences), a networked training using such an information can not be practically used to provide real-time predictions. To address this issue, one needs to implement causal filters within a deep learning architecture. The basic approach in this regard is to train the model without any restrictions on causality and during the implementation phase, mask those sections of the filter kernel that require future values as input. This masking approach can be achieved by setting the associated parts of the filter kernel to zero at each stochastic gradient decent (SGD) update. This approach is, however, costly in terms of required/wasted computational resources as, more-or-less, half of the multiplication and addition operations are wasted. In the BP-Net architecture we utilize an alternative approach, i.e., the *Casual Convolutions* [37] are incorporated within the BP-Net architecture. Fig. 3 illustrates one example of casual convolutions. In causal convolutions, by capitalizing on the translation-equivariance property of the convolution, the input signal is first shifted and padded by the kernel size and then the introduced shifting is removed.

For long sequences, architectures with causal convolutions are much faster to train than RNNs due to absence of recurrent connections. However, one of the main drawbacks of the models with casual convolutions is limited receptive field. For example, in Fig. 3, the receptive field of the neurons at the output layer is only 4, i.e., they see effects from upto four previous input samples

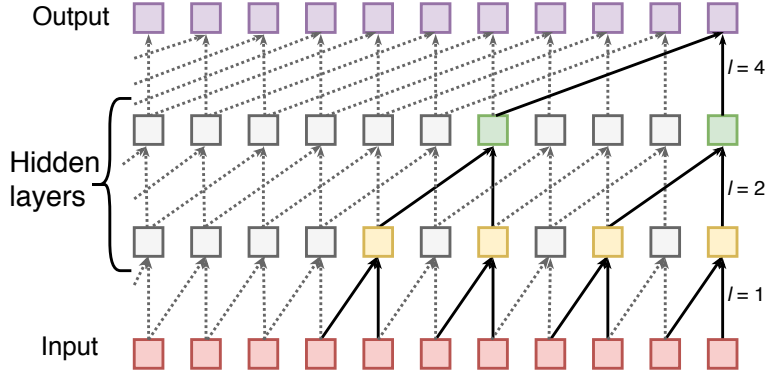


Figure 4: An example of a Dilated Causal Convolution.

(limited history size). For increasing the receptive field in casual convolutions, very deep networks or large filters should be applied, which are not generally feasible approaches. To address this issue, therefore, dilated convolutions [40] are used within the BP-Net architecture as described below.

Dilated Convolutions: Dilated convolutions are used as an effective way to enlarge the receptive field within the BP-Net without losing resolution. Consider a 1-D time series $\mathbf{x} \in \mathbb{R}^{N_x}$ and a 1-D Kernel $\mathcal{K} : \{0, 1, \dots, R-1\} \rightarrow \mathbb{R}$ with size R . Discrete dialated convolution operation $D(p)$ on the p^{th} element of vector \mathbf{x} with dilation rate L is defined as follows

$$D(p) \triangleq (\mathbf{x} *_L \mathcal{K})(p) = \sum_{i=0}^{R-1} \mathcal{K}(i) \times \mathbf{x}(p - L \times i), \quad (1)$$

where dialated convolution is denoted by $*_L$, and $(p - L \times i)$ refers to elements of the input vector \mathbf{x} prior to time p^{th} element. Fig. 4 provides an illustration of dilated convolution. The dilation rate (L) is a design parameter, and dilated convolution becomes similar to the regular convolution with dilation rate of $L = 1$. Generally speaking, in dilated convolution, the receptive field of a kernel \mathcal{K} with size R is expanded to $R + (R - 1)(L - 1)$ with dilated stride of L .

Residual Connections In theory, by stacking more layers, we expect that the network achieves lower training error and learn better, however, in the reality, it is very challenging to train very deep neural networks because of vanishing and exploding gradient problems. In other words, by adding more layers in a deep neural network, accuracy gets saturated, and then degrades promptly. This problem is called “degradation”, which was introduced by [38]. In [38], the authors, addressed the degradation problem by adding shortcut connections to the network referred to as “residual connections”. In this case, by skipping over some layers, information passes into the network.

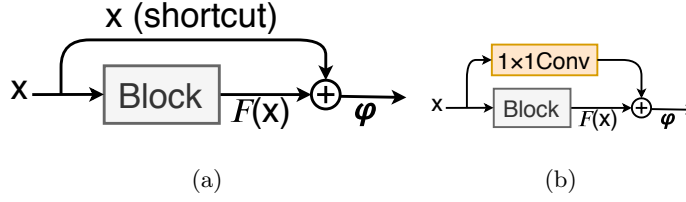


Figure 5: Residual learning (a) Identity block. (b) Convolutional block.

Fig. 5(a) shows a sample of “Identity Block” which is a standard block used in ResNets. This block is used when the dimensions of the input and the output are the same. In the case that the input and output dimensions do not match, another type of ResNets blocks called “Resnet Convolutional Block” are employed to match dimensions (done by 1×1 convolutions) as shown in Fig. 5(b). It is noteworthy to mention that in Fig. 5, φ represents the activation function, which applied on the element-wise addition of residual mapping function (F) and the input (x).

3.4. BP-Net Structure and Hyperparameters Settings

In the first step, the following nonlinear μ -law transformation is applied to normalize the input data

$$F(X) = \text{sign}(X) \frac{\ln(1 + \mu|X|)}{\ln(1 + \mu)}. \quad (2)$$

It is noteworthy to note that such μ -law transformation is used as a transformation to quantize data in previous works such as [37]. Inspired by Reference [39], the residual block as a basic block is used for the network structure (Fig. 6). This block consists of two dilated casual convolutions and two nonlinear activation function (ELU) [41]. Moreover, dropout [42] for regularization, and weight normalization [43] are used in this block. We use Adam optimizer as the optimization algorithm with learning rate set to 0.001. The learning rate changes in a cycle with the length of 100 epochs. After 20 epochs, we divide learning rate by 2, but after 100 epochs instead of dividing by 2, we multiply it by 14.4. Therefore, the learning rate at the beginning of each cycle will be 90% of the learning rate at the beginning of the previous cycle. This novel approach of creating learning rate causes to avoid being stuck in local minimums while speeding the training of the architecture. These models are trained with a mini-batch size of 64. The exact structure of the proposed BP-Net network is as follows:

- PPG and ECG signal as inputs are separately fed to a 1×1 convolutions layer with 32 kernels, and then the concatenated channel-wise results are fed to the first residual block.

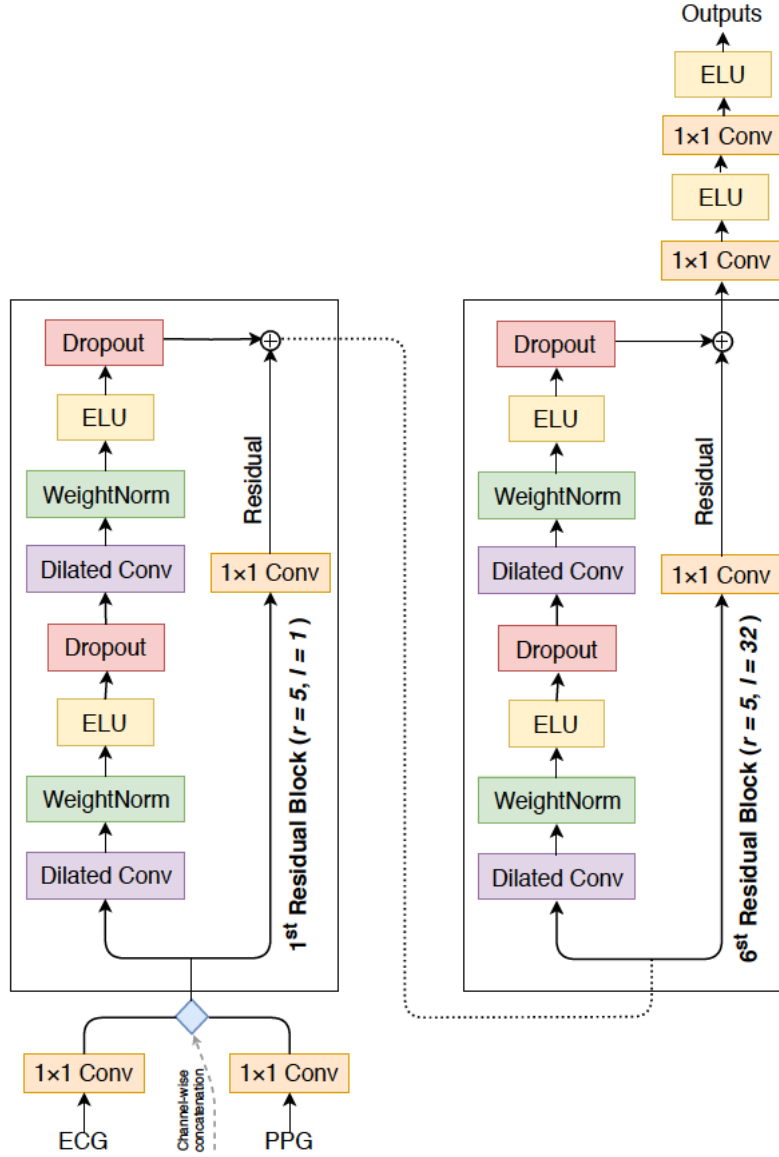


Figure 6: The architecture of proposed BP-Net.

- Six residual blocks are stacked in the proposed architecture with the following characteristics:
 - All of dilated causal convolutions have kernel size of 5.
 - The dilation factor (L) is doubled for every layer, i.e., 1, 2, 4, 8, 16, and 32.
 - For Residual block 1 to 6, the number of kernels are 32, 32, 64, 64, 128, and 256, respectively.
- The output of the sixth block is fed to a 1×1 convolution layer with 256 kernels following

Table 1: The RMSE/MAE between actual BP(SBP, DBP) and estimated BP in the proposed model.

	Average RMSE (mmHg)	Average MAE (mmHg)	RMSE (mmHg)	MAE (mmHg)
SBP	3.23 ± 2.11	2.76 ± 1.92	3.77	2.7
DBP	1.57 ± 1.12	1.30 ± 0.93	1.86	1.26

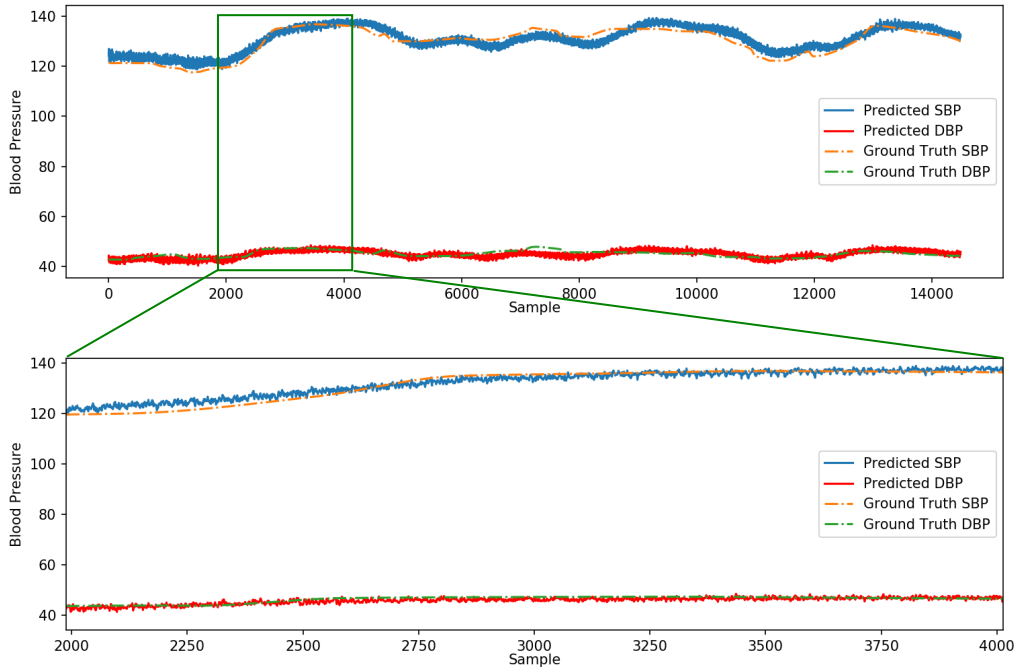


Figure 7: Continuous BP measurement.

by ELU activation function, (1×1) convolution layer with 2 kernels, and again an ELU activation function.

This completes presentation of the proposed BP-Net architecture. Next, we present experimental results to evaluate performance of the proposed architecture.

4. Experiments and Results

In this section, we present different experimental results based on real-data sets to evaluate performance of the proposed continuous BP estimation architecture. Details of the constructed dataset is described in Section 3. Fig. 7 shows the continuous SBP and DBP tracking of an individual using the proposed BP-Net architecture. From this figure, it is observed that the proposed

model is capable of reliably tracking continuous SBP and DBP. To measure the accuracy of the proposed architecture, commonly used evaluation metrics, i.e., the root mean square error (RMSE) and the mean absolute error (MAE), are used given by

$$\text{RMSE} = \sqrt{\frac{1}{n} \sum_{j=1}^n |B_j - \hat{B}_j|^2}, \quad \text{and} \quad \text{MAE} = \frac{1}{n} \sum_{j=1}^n |B_j - \hat{B}_j|, \quad (3)$$

where B_j is the actual observed BP, whereas \hat{B}_j determines its corresponding predicted value. Table 1, summarizes the average RMSE and MAE results obtained from averaging individual RMSE and MAE values corresponding to each subject (104 subjects). Table 1 also illustrates the combined MAE and RMSE results obtained by stacking together the target signals of all the subjected. The overall results presented in Table 1 shows exceptional performance of the proposed BP estimation framework especially for estimating the DBP.

It is worth mentioning that in contrary to existing BP estimation solutions, the proposed framework, provides continuous SBP and DBP outputs for all samples. Intuitively speaking, output of the proposed framework can be considered as upper and lower bounds on the BP signal computed at all time samples. As a side note to our discussion, we would like to point out that due to absence of a standard dataset, fair comparison with existing works is not straightforward.

4.0.1. The BP Error Histogram Analysis

To determine reliability of the proposed BP-Net architecture, histogram of the BP estimation error for DBP and SBP is shown in Fig. 8(a)-(b). It is evident that the distribution of estimation error histogram can be modelled as a Gaussian function with approximately zero mean. As expected, standard deviation of the SBP error histogram is greater than that of the DBP, since the variance of the SBP target histogram is much larger than the DBP target histogram in database Fig. 1.

4.1. Evaluation using AAMI Standards and BHS Standards

To evaluate robustness and accuracy of the proposed architecture, the model is evaluated on two common standards namely the Association for the Advancement of Medical Instrumentation (AAMI) [44] and the British Hypertension Society Standard (BHS) [45]. Moreover, in the following subsections, we investigate performance of the proposed BP-Net architecture by using Bland-Altman test, and Pearson's correlation coefficient analysis.

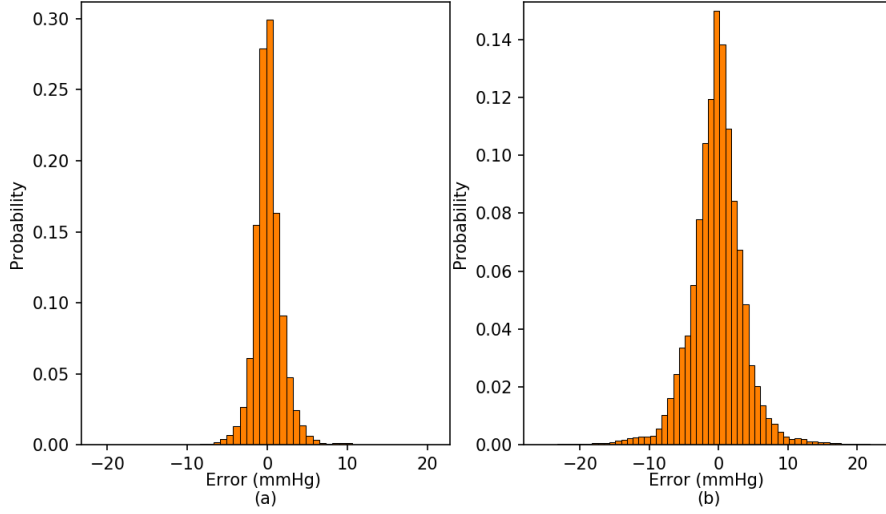


Figure 8: (a) DBP error histogram of the proposed architecture. (b) SBP error histogram of the proposed architecture.

Table 2: Comparison of the proposed model with the AAMI standard.

		Subjects	ME (mmHg)	STD (mmHg)
The BP-Net Architecture	SBP	104	0.2774	3.77
	DBP	104	0.0771	1.86
AAMI standard	SBP & DBP	≥ 85	≤ 5	≤ 8

Table 3: Comparison of the proposed model with BHS standard.

		Cumulative Error Percentage		
		≤ 5 mmHg	≤ 10 mmHg	≤ 15 mmHg
The BP-Net Architecture	SBP	94.01%	99.06%	99.78%
	DBP	98.78%	99.92%	100.00%
BHS standard	grade A	60%	85%	95%
	grade B	50%	75%	90%
	grade C	40%	65%	85%

According to the AAMI standard, the BP measurement devices should have mean error (ME) and standard deviation of error (SDE) values lower than 5 and 8 mmHg, respectively [44]. Table 2 shows the ME and SDE computed based on the overall results obtained from the proposed methodology. It can be observed that the proposed framework have ME and SDE values much lower than

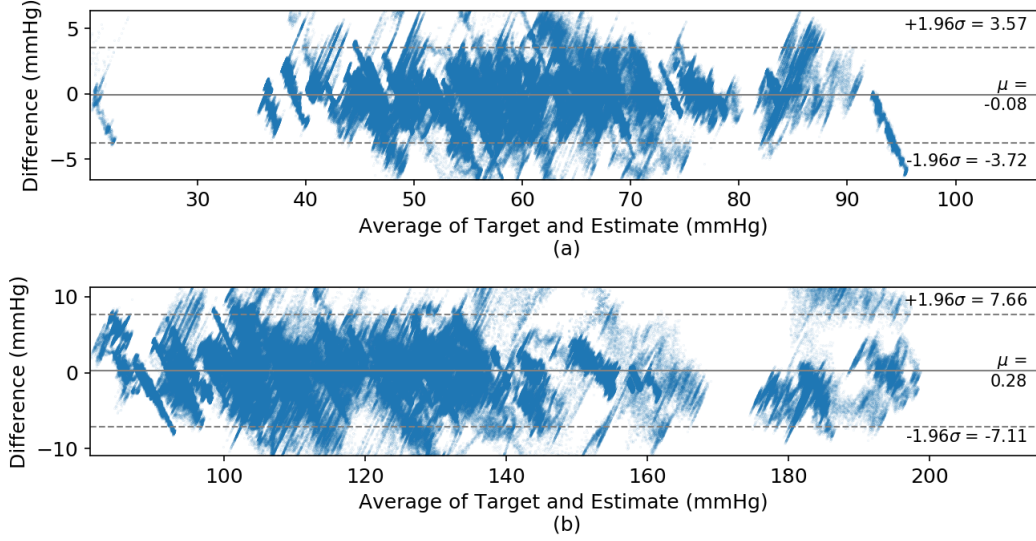


Figure 9: Bland-Altman plot of (a) The DBP, and; (b) The SBP. The limits of agreement (LOA) for DBP and SBP are $[-3.72, 3.57]$ and $[-7.11, 7.66]$, respectively.

the acceptable ME and SDE requirements of the AAMI standard. The other requirement of the AAMI standard is that the device should be evaluated on a population more than 85 subjects [2], which is also satisfied in this work (104 subjects).

The BHS standard [45] grades BP measurement devices based on their cumulative percentage of errors lower than three different thresholds of 5, 10, and 15 mmHg. Table 3 illustrates that not only the obtained results meet the requirements of the BHS standard, but also the grade of estimation for both DBP and SBP is equal to *A* grade. Moreover, as shown in Table 3, more than 94% of the estimated targets have cumulative error less than 5 mmHg showing the exceptional performance of the proposed model.

4.2. Statistical Analysis

Fig. 9 shows the Bland-Altman plot of the SBP and the DBP estimation. For the proposed BP-Net architecture, the limits of agreement $[\mu - 1.96\sigma, \mu + 1.96\sigma]$ for SBP and DBP have been found to be $[-7.11, 7.66]$ and $[-3.72, 3.57]$ respectively. This means that 95% of the estimated SBPs have error less than 7.73 mmHg and 95% of the measured DBPs have error less than 4.05 mmHg, which indicates that the model provides acceptable estimates.

Finally, Figs. 10(a)-(b) illustrate the regression plot for SBP and DBP estimation. The Pearson

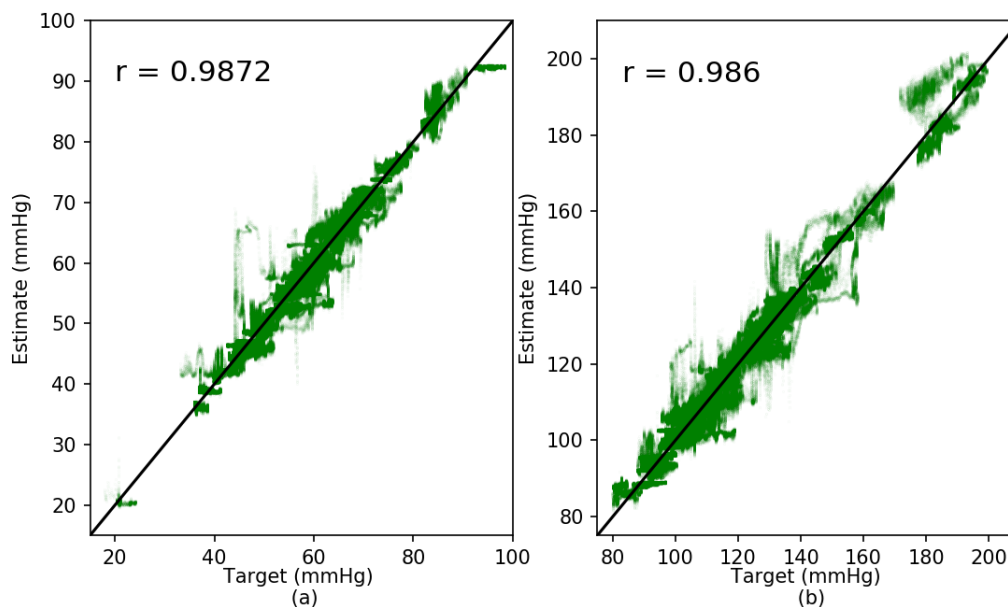


Figure 10: The regression plot for (a) The DBP, and; (b) The SBP. The Pearson's correlation coefficients are $r = 0.9872$ and $r = 0.986$ for DBP and SBP, respectively.

correlation coefficients of DBPs and SBPs are $r = 0.9872$ and $r = 0.986$, respectively. Both of the coefficients are very close to 1.0 indicating high linearity between the target and estimated BP.

5. Conclusion

Inevitable increase in the population of seniors, makes continuous BP monitoring essential as it provides invaluable information about individuals' cardiovascular conditions. The paper first identifies two key drawbacks associated with the existing continuous BP estimation models, i.e., (i) Relying heavily on extraction of hand-crafted features, i.e., ignoring the real potential of deep learning in utilization of the intrinsic features (deep features) and instead using representative hand-crafted features prior to extraction of deep features, and; (ii) Lack of a benchmark dataset for evaluation and comparison of developed deep learning-based BP estimation algorithms. To alleviate these issue, the paper proposes an efficient algorithm, referred to as the BP-Net, based on the deep learning techniques for the continuous, cuff-less, and calibration-free of systolic and diastolic BP. In the proposed BP-Net architecture, raw ECG and PPG signals as utilized without extraction of PAT features, to explore the real potential of deep learning in utilization of intrinsic features (deep

features). The proposed BP-Net architecture is more accurate than canonical recurrent networks and enhances the long-term robustness of the BP estimation task. Furthermore, by capitalizing on the significant importance of continuous BP monitoring and the fact that datasets used in recent literature are not unified and properly defined, a benchmark data set is constructed from the MIMIC-I and MIMIC-III databases to provide a unified base for evaluation and comparison of deep learning-based BP estimation algorithms. The proposed BP-Net architecture is evaluated based on this benchmark data-set demonstrating promising results and shows generalizable capability to multiple subjects.

References

- [1] “World Population Ageing,” *Department of Economics and Social Affairs, Population Division*, United Nations, 2017.
- [2] M. Kachuee, M.M. Kiani, H. Mohammadzade, M. Shabany, “Cuffless Blood Pressure Estimation Algorithms for Continuous Health-care Monitoring,” *IEEE Trans. Biomed. Eng.*, vol. 64, no. 4, pp. 859-869, 2017.
- [3] W.H. Lin, F. Chen, Y. Geng, N. Ji, P. Fang, and G. Li, “Towards Accurate Estimation of Cuffless and Continuous Blood Pressure using Multi-order Derivative and Multivariate Photoplethysmogram Features,” *Biomedical Signal Processing and Control*, 63, p.102198., 2021.
- [4] M.R. Mohebbian, A. Dinh, K. Wahid, and M.S. Alam, “Blind, cuff-less, Calibration-free and Continuous blood Pressure Estimation using Optimized Inductive Group Method of Data Handling” *Biomedical Signal Processing and Control*, 57, p.101682, 2020.
- [5] A. Chandrasekhar, *et al.*, “Smartphone-based Blood Pressure Monitoring via the Oscillometric Finger-pressing Method,” *Sci. Transl. Med.*, vol. 10, 2018.
- [6] F. Miao, Z. Liu, J. Liu, B. Wen and Y. Li, “Multi-sensor Fusion Approach for Cuff-less Blood Pressure Measurement,” *IEEE J. Biomed. & Health Inf.*, 2019. In Press.
- [7] C. El-Hajj, and P.A. Kyriacou, “A Review of Machine Learning Techniques in Photoplethysmography for the Non-invasive Cuff-less Measurement of Blood Pressure,” *Biomedical Signal Processing and Control*, vol. 58, pp. 101870, 2020.
- [8] Y. Qiu, *et al.*, “Cuffless Blood Pressure Estimation based on Composite Neural Network and Graphics Information,” *Biomedical Signal Processing and Control*, vol. 70, 2021.
- [9] M.S. Tanveer, and M.K. Hasan, “Cuffless Blood Pressure Estimation from Electrocardiogram and Photoplethysmogram using Waveform based ANN-LSTM Network”, *Biomedical Signal Processing and Control*, vol. 51, pp. 382-392, 2019.
- [10] B. Zhang, J. Ren, Y. Cheng, B. Wang and Z. Wei, “Health Data Driven on Continuous Blood Pressure Prediction Based on Gradient Boosting Decision Tree Algorithm,” *IEEE Access*, vol. 7, pp. 32423-32433, 2019.

- [11] S.G. Khalid, J. Zhang, F. Chen, D. Zheng, “Blood Pressure Estimation using Photoplethysmography Only: Comparison Between Different Machine Learning Approaches,” *J. Healthc. Eng.*, pp. 1-13, 2018.
- [12] M. Simjanoska, M. Gjoreski, M. Gams, A.M. Bogdanova, “Non-invasive Blood Pressure Estimation from ECG using Machine Learning Techniques,” *Sensors*, vol. 18, no. 4, 2018.
- [13] S.K. Berkaya, A.K. Uysal, E.S. Gunal, S. Ergin, S. Gunal, and M.B. Gulmezoglu, “A Survey on ECG Analysis”, *Biomedical Signal Processing and Control*, vol. 43, pp. 216-235, 2018.
- [14] F.P.W. Lo, C.X.T. Li, J. Wang, J. Cheng, and M.Q.H. Meng, “Continuous Systolic and Diastolic Blood Pressure Estimation Utilizing Long Short-Term Memory Network,” *IEEE Int. Conf. Eng. in Med. & Biol. Society (EMBC)*, pp. 1853-1856, 2017.
- [15] H. Xiao, M. Butlin, I. Tan, A. Qasem and A. P. Avolio, “Estimation of Pulse Transit Time From Radial Pressure Waveform Alone by Artificial Neural Network,” *IEEE J. Biomed. & Health Inf.*, vol. 22, no. 4, pp. 1140-1147, July 2018.
- [16] Y. Ma, *et al.* “Relation between Blood Pressure and Pulse Wave Velocity for Human Arteries,” *Proceedings of the National Academy of Sciences*, vol. 115, no. 44, pp. 11144-11149, 2018.
- [17] T.H. Huynh, R. Jafari, W.Y. Chung, “Noninvasive Cuffless Blood Pressure Estimation using Pulse Transit Time & Impedance Plethysmography,” *IEEE Trans. Biomed. Eng.*, vol. 66, no. 4, pp. 967-976, 2019.
- [18] R. Mukkamala, and J.O. Hahn, “Toward Ubiquitous Blood Pressure Monitoring via Pulse Transit Time: Predictions on Maximum Calibration Period and Acceptable Error Limits,” *IEEE Trans. Biomed. Eng.*, vol. 65, no. 6, pp. 1410-1420, 2018.
- [19] S. Ahmad, *et al.* “Electrocardiogram-assisted Blood Pressure Estimation,” *IEEE Trans. Biomed. Eng.*, vol. 59, no. 3, pp. 608-618, 2012.
- [20] J.M. Huttunen, L. Kärkkäinen, and H. Lindholm, “Improving Pulse Transit Time Estimation of Aortic PWV and Blood Pressure using Machine Learning and Simulated Training Data,” *arXiv preprint arXiv*, 1903.02262, 2019.
- [21] Y. Yoon *et al.*, “Cuff-Less Blood Pressure Estimation Using Pulse Waveform Analysis and Pulse Arrival Time,” *IEEE J. Biomed. & Health Inf.*, vol. 22, no. 4, pp. 1068-1074, July 2018.
- [22] Z. Tang *et al.*, “A Chair-Based Unobtrusive Cuffless Blood Pressure Monitoring System Based on Pulse Arrival Time,” *IEEE J. Biomed. & Health Inf.*, vol. 21, no. 5, pp. 1194-1205, Sept. 2017.
- [23] H. Gesche, D. Grosskurth, G. Kuchler, and A. Patzak, “Continuous Blood Pressure Measurement by using the Pulse Transit Time: Comparison to a Cuff-based Method,” *European J. Applied Physiology*, vol. 112, no. 1, pp. 309-315, 2012.
- [24] I. Sharifi, S. Goudarzi, and M.B. Khodabakhshi, “A Novel Dynamical Approach in Continuous Cuffless Blood Pressure Estimation based on ECG and PPG Signals,” *Artificial Intell. Medic.*, pp. 143-151, 2019.
- [25] A. Strin, “Improvements in Indirect Blood Pressure Estimation via Electrocardiography and Photoplethysmography,” 2016.
- [26] M. Rehman, *et al.*, “Multiday EMG-based Classification of Hand Motions with Deep Learning Techniques,” *Sensors*, vol. 18, no. 8, 2018.
- [27] P. Su, X.R. Ding, Y.T. Zhang, J. Liu, F. Miao, and N. Zhao, “Long-term Blood Pressure Prediction with Deep

- Recurrent Neural Networks,” *IEEE EMBS International Conference on Biomedical and Health Informatics (BHI)*, pp. 323-328, 2018.
- [28] S. Lee, and J.H. Chang, “Oscillometric Blood Pressure Estimation based on Deep Learning,” *IEEE Trans. Ind. Informat.*, vol. 13, no. 2, pp. 461-472, 2017.
- [29] M.S. Tanveer, and M.K. Hasan, “Cuffless Blood Pressure Estimation from Electrocardiogram and Photoplethysmogram using Waveform based ANN-LSTM Network,” *Biomedical Signal Processing and Control*, vol. 51, no. 1, pp. 382-392, 2019.
- [30] A.L. Goldberger, L.A. Amaral, L. Glass, J.M.Hausdorff, P.C. Ivanov, R.G. Mark, J.E. Mietus, G.B. Moody, C.K. Peng, and H.E. Stanley, “PhysioBank, PhysioToolkit, and PhysioNet: Components of a New Research Resource for Complex Physiologic Signals,” *Circulation*, vol. 101, no. 23, pp. e215-e220, 2000.
- [31] S. Banerjee, R. Gupta, and M. Mitra, “Delineation of ECG Characteristic Features using Multiresolution Wavelet Analysis Method,” *Measurement*, vol. 45, no. 3, pp. 474-487, 2012.
- [32] H. Limaye, and V.V. Deshmukh, “ECG Noise Sources and Various Noise Removal Techniques: A Survey,” *Int. J. Application or Innovation in Engineering and Management*, vol. 5, no. 2, pp. 86-92, 2016.
- [33] R. Vullings, B. De Vries, and J.W. Bergmans, “An Adaptive Kalman Filter for ECG Signal Enhancement,” *Computers in Cardiology*, vol. 58, no. 4, pp. 1094-1103, 2011.
- [34] O. Sayadi, and M.B. Shamsollahi, “ECG Denoising and Compression using a Modified Extended Kalman Filter Structure,” *IEEE Trans. Biomed. Eng.*, vol. 55, no. 9, pp. 2240-2248, 2008.
- [35] C. Haritha, M. Ganesan, and E.P. Sumesh, “A Survey on Modern Trends in ECG Noise Removal Techniques,” *Int. Conf. Circuit, Power & Computing Technologies (ICCPCT)*, pp. 1-7, 2016.
- [36] P. Karthikeyan, M. Murugappan, and S. Yaacob, “ECG Eignal Denoising using Wavelet Thresholding Techniques in Human Stress Assessment,” *Int. J. Electr. Eng. & Informat.*, vol. 4, no. 2, p. 306, 2012.
- [37] A.V.D. Oord and *et al.* “Wavenet: A Generative Model for Raw Audio,” *ArXiv preprint arXiv:1609.03499*, 2016.
- [38] K. He, X. Zhang, S. Ren, and J. Sun, “Deep Residual Learning for Image Recognition,” *IEEE Conf. Comput. Vision & Pattern Recognition*, pp. 770-778, 2016.
- [39] S. Bai, J. Z. Kolter, and V. Koltun, “An Empirical Evaluation of Generic Convolutional and Recurrent Networks for Sequence Modeling,” *arXiv preprint arXiv*, 1803.01271, 2018.
- [40] T. Sercu and G. Vaibhava, “Dense Prediction on Sequences with Time-Dilated Convolutions for Speech Recognition,” *arXiv preprint arXiv:1611.09288*, 2016.
- [41] D. A. Clevert, T. Unterthiner, and S. Hochreiter, “Fast and Accurate Deep Network Learning by Exponential Linear Units (ELUS),” *arXiv preprint arXiv:1511.07289*, 2015.
- [42] N. Srivastava, G. Hinton, A. Krizhevsky, I. Sutskever, R. Salakhutdinov, “Dropout: A Simple Way to Prevent Neural Networks from Overfitting,” *J. Machine Learning Research*, vol. 15, no. 1, pp. 1929-1958, 2014.
- [43] T. Salimans and D. P. Kingma, “Weight Normalization: A Simple Reparameterization to Accelerate Training of Deep Neural Networks,” *Advances in Neural Information Process. Sys.*, pp. 901-909, 2016.
- [44] Association for the Advancement of Medical Instrumentation, “American National Standards for Electronic or Automated Sphygmomanometers,” *ANSI/AAMI SP 10-1987*, 1987.

- [45] E. O'Brien *et al.*, "The British Hypertension Society Protocol for the Evaluation of Automated and Semi-automated Blood Pressure Measuring Devices with Special Reference to Ambulatory Systems," *J. hypertension*, vol. 8, no. 7, pp. 607-619, 1990.